

Azalysine Analogues as Probes for Protein Lysine Deacetylation and Demethylation

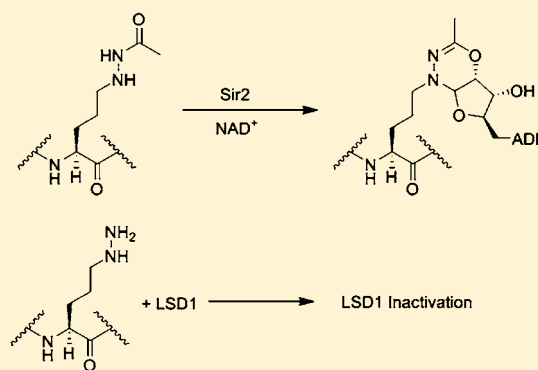
Blair C. R. Dancy,[†] Shonoi A. Ming,[†] Romeo Papazyan,[†] Christine A. Jelinek,[†] Ananya Majumdar,[‡] Yan Sun,[†] Beverley M. Dancy,[†] William J. Drury, III,[†] Robert J. Cotter,[†] Sean D. Taverna,[†] and Philip A. Cole^{*,†}

[†]Department of Pharmacology and Molecular Sciences, Johns Hopkins School of Medicine, Baltimore, Maryland 21205, United States

[‡]The Johns Hopkins Biomolecular NMR Center, Johns Hopkins University, Baltimore, Maryland 21218, United States

S Supporting Information

ABSTRACT: Reversible lysine acetylation and methylation regulate the function of a wide variety of proteins, including histones. Here, we have synthesized azalysine-containing peptides in acetylated and unacetylated forms as chemical probes of the histone deacetylases (HDAC8, Sir2Tm, and SIRT1) and the histone demethylase, LSD1. We have shown that the acetyl-azalysine modification is a fairly efficient substrate for the sirtuins, but a weaker substrate for HDAC8, a classical HDAC. In addition to deacetylation by sirtuins, the acetyl-azalysine analogue generates a novel ADP-ribose adduct that was characterized by mass spectrometry, Western blot analysis, and nuclear magnetic resonance spectroscopy. This peptide-ADP-ribose adduct is proposed to correspond to a derailed reaction intermediate, providing unique evidence for the direct 2'-hydroxyl attack on the *O*-alkylimidate intermediate that is formed in the course of sirtuin catalyzed deacetylation. An unacetylated azalysine-containing H3 peptide proved to be a potent inhibitor of the LSD1 demethylase, forming an FAD adduct characteristic of previously reported related structures, providing a new chemical probe for mechanistic analysis.



INTRODUCTION

Post-translational modifications (PTMs), such as acetylation, methylation, phosphorylation, ADP-ribosylation, and ubiquitinylation of proteins are critical to cell function.^{1,2} These modifications can exert influence on a protein's stability, enzymatic activity, or ability to interact with other proteins or molecules, such as DNA.^{3,4} Many proteins, such as histones and the tumor suppressor protein p53, have residues that can be modified in a variety of ways.⁵ Their lysines, in particular, can be modified by a diverse array of PTMs, with each state having a potentially distinct impact on protein function.^{2,5} For example, when the Lys-382 residue in the p53 C-terminus is acetylated, the protein is stabilized and p53-mediated transcription increases.^{6–9} In contrast, methylation or ubiquitinylation at Lys-382 both attenuate p53-mediated transcription and the latter can direct the protein for proteasome-mediated degradation.^{6–9} In this way, the opposing functions of these modifications and the interplay of the proteins that install and remove such chemical modifications help provide a framework for regulating normal cell growth, differentiation, and epigenetic phenomena.¹⁰ The dysregulation of these pathways can result in human disease, implicating the responsible machinery as potential drug targets.¹¹ Accordingly, detailed mechanistic understanding of enzymes that either add or remove PTMs

promises to yield key insights that will further aid in the design of specific inhibitors and treatments.

Lysine deacetylation is regulated by a group of enzymes known as histone deacetylases (HDACs) (Figure 1a), which are established targets in cancer and are under investigation for their roles in other diseases.^{12–17} There exist two families of HDACs, the classical metallohydrolases that directly hydrolyze the acetamide function, and the sirtuins, unusual enzymes that cleave acetyl groups through the involvement of the NAD cofactor. In sirtuin deacetylation reactions, NAD is consumed to afford nicotinamide, deacetylated peptide, and the metabolite, 2'-*O*-acetyl-ADP-ribose.^{18–22} As would be expected for enzymes that modulate protein acetylation, both classical HDACs and sirtuins are involved in many cellular processes, including transcriptional regulation, cell division, and apoptosis.^{23–26}

To better understand HDAC activity, intensive efforts have been made to develop chemical probes that interrogate their mechanisms and function.^{16,27–30} Many of these probes have proved useful in the study of sirtuin deacetylation.^{18,31–36} Acetyl-lysine analogues (Figure 2a), including methanesulfon-

Received: October 13, 2011

Published: February 21, 2012

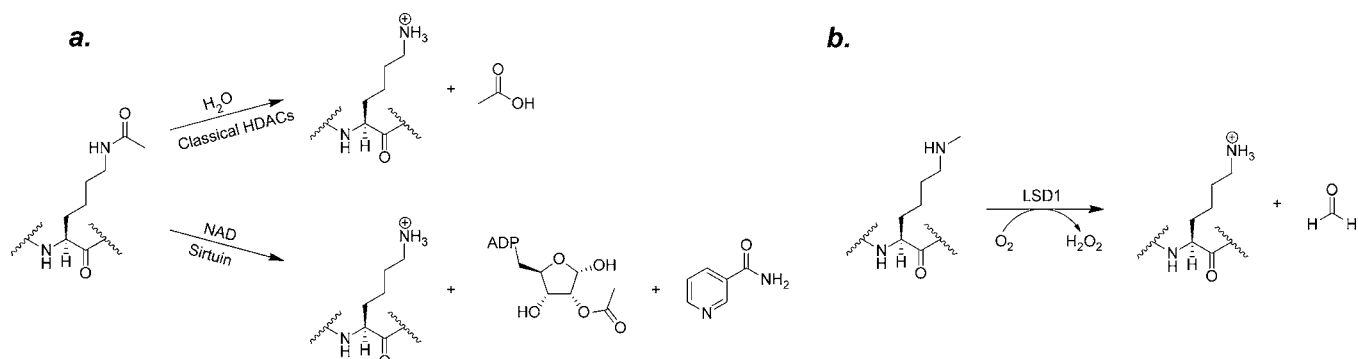


Figure 1. (a) Schematic of deacetylation by either classical HDACs or sirtuins; (b) schematic of lysine-specific demethylation by the flavin-dependent amine oxidase, LSD1.

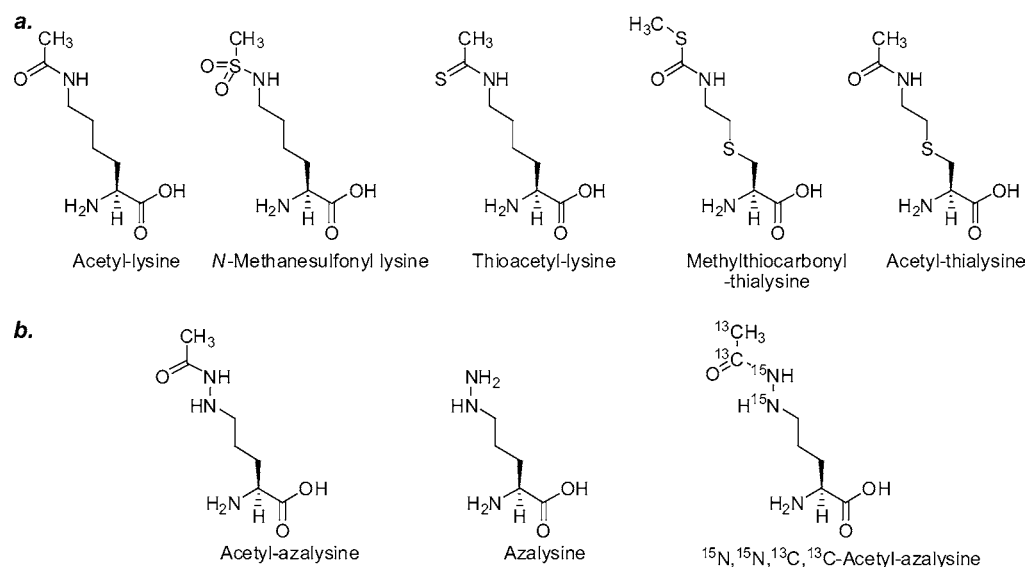


Figure 2. (a) Schematic of acetyl-lysine analogues; (b) schematic of analogues presented in this manuscript.

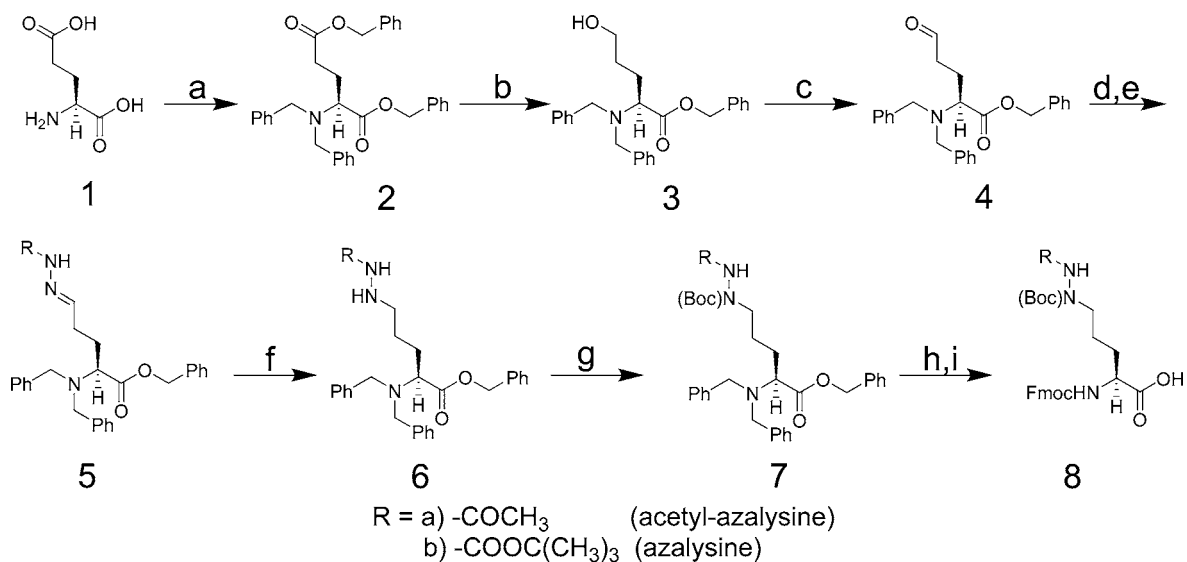


Figure 3. Synthetic scheme for the synthesis of Fmoc-acetyl-(Boc)-azalysine and Fmoc-(Boc)₂-azalysine. Synthesis of compounds 1–4 performed as was previously described.⁵² (a) Benzyl bromide, H₂O, K₂CO₃, NaOH, reflux; (b) diisobutylaluminum hydride, THF, 0 °C; (c) Swern oxidation, –78 °C; (d) *t*-butylcarbazate, THF, rt, or (e) acetic hydrazide, THF, rt; (f) sodium cyanoborohydride, AcOH, EtOH, rt; (g) di-*t*-butyl dicarbonate, dimethylaminopyridine, CH₂Cl₂, rt; (h) palladium black, HCOOH, MeOH, rt; (i) 9-fluorenylmethyl succinimidyl carbonate, 1,4-dioxane, K₂CO₃, 0 °C.

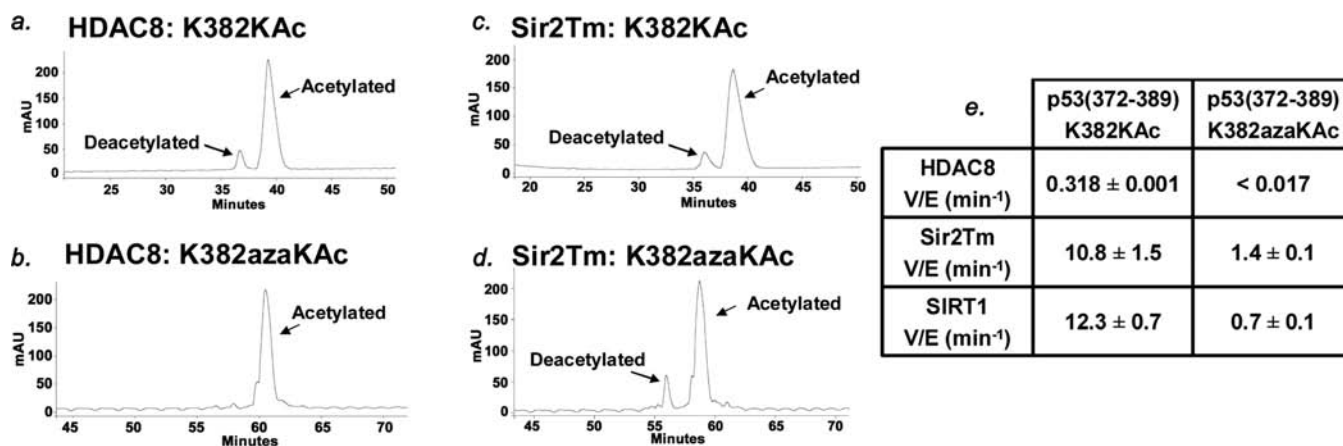


Figure 4. MALDI HPLC deacetylation assays of: (a) HDAC8 and K382KAc-containing p53 peptide; (b) HDAC8 and K382azaKAc-containing p53 peptide; (c) Sir2Tm and K382KAc-containing p53 peptide; (d) Sir2Tm and K382azaKAc-containing p53 peptide; (e) and summary of kinetic turnover data.

yl-, methylthiocarbonyl thia-, acetyl-thia-, and thioacetyl-lysine have not only been useful in studying the sirtuin mechanism, but also in providing insight into PTM function.^{37–42} Thioacetyl-lysine, in particular, has been invaluable in understanding the novel mechanism by which the sirtuins deacetylate the acetyl-lysine moiety. This analogue leads to the generation of a trapped alkylimidate adduct with ADP-ribose, thought to represent a catalytic intermediate.^{43–45}

Methylation of lysine residues is another reversible process that plays a major role in chromatin remodeling and transcriptional regulation.⁴⁶ Methyl groups that are installed by either the SET domain- or non-SET domain-containing methyl transferases can be enzymatically removed by demethylases, such as lysine-specific demethylase 1 (LSD1) or the JmjC domain-containing demethylases (Figure 1b).^{47–49} LSD1 uses the FAD cofactor and molecular O₂ to demethylate methyl-lysine residues, liberating formaldehyde, hydrogen peroxide, and the demethylated peptide.

Lysine analogues containing propargyl, chlorovinyl, and hydrazine functionalities have been developed as LSD1 demethylase mechanism-based inhibitors.^{50,51} The prior hydrazine analogue of lysine, a highly potent LSD1 inhibitor, extends the side-chain by an extra atom relative to natural lysine. Inspired by this prior work, we considered the possibility that a better lysine analogue isostere, azalysine (Figure 2b), could prove an interesting mechanistic probe of lysine-modifying enzymes, both LSD1, and if acetylated, HDACs. Here, we describe our efforts to synthesize acetyl-azalysine and azalysine, incorporate them into peptides, and assess how these analogues are processed by HDACs and the LSD1 demethylase.

RESULTS

Synthesis of Acetyl-Azalysine and Azalysine. Our initial ambition was to synthesize acetyl-azalysine in a suitably protected form for use in solid phase peptide synthesis via the Fmoc strategy. This acetyl-azalysine analogue involves the replacement of the ϵ -carbon of acetyl-lysine with a nitrogen atom (Figure 2b), and is an acetyl-lysine isostere with distinct electronic properties that we predicted, because of the alpha-effect,⁵³ might form a stable adduct with ADP-ribose in the sirtuin reaction. We began this synthesis (Figure 3) using known procedures to convert L-glutamic acid (**1**) to the

corresponding perbenzylated-aldehyde (**4**).⁵² This molecule was then condensed with acetic hydrazide to give the corresponding hydrazone precursor (**5a**) for acetyl-azalysine. The hydrazone was then reduced with sodium cyanoborohydride^{54,55} to yield hydrazide **6a**. For use in solid-phase peptide synthesis, the free secondary ϵ -nitrogen was protected with a Boc group using di-*t*-butyl dicarbonate, yielding compound **7a**. The benzyl protecting groups were efficiently removed using catalytic transfer hydrogenation with palladium black,⁵⁶ and the α -amino group was converted to the Fmoc derivative (**8a**) using Fmoc-*O*-succinimide. The unacetylated azalysine precursor (**8b**) was afforded via a slightly modified strategy in which the terminal nitrogen was protected by Boc. The synthesized acetyl-azalysine and azalysine building blocks (**8**) were then incorporated into separate p53 peptides comprising residues (372–389), with the modified residues substituting for known acetylation site Lys-382 to yield K382azaKAc (Supporting Information Figure S1a) or K382azaK (Supporting Information Figure S1b), respectively.

K382azaKAc p53 Peptide As a Histone Deacetylase Substrate. Having created the modified peptides, we then proceeded to evaluate the ability of HDAC8, a classical HDAC, Sir2Tm, a bacterial sirtuin, and SIRT1, a human sirtuin, to deacetylate the acetyl-azalysine moiety in K382azaKAc by using an HPLC-based assay (Figure 4a–d), analogous to a method that has been previously described.³⁸ Our data (Figure 4e) show that the acetyl-azalysine functionality can be minimally cleaved by HDAC8, with deacetylation of K382azaKAc showing >20-fold reduction in efficiency compared with the corresponding natural acetylated substrate, K382KAc (apparent $k_{\text{cat}} = 0.318 \pm 0.001 \text{ min}^{-1}$). Sir2Tm and SIRT1 deacetylation of K382azaKAc was somewhat more robust (1.4 ± 0.1 and $0.7 \pm 0.1 \text{ min}^{-1}$, respectively), 8- and 18-fold, respectively, relative to natural substrate (10.8 ± 1.5 and $12.3 \pm 0.7 \text{ min}^{-1}$, respectively).

We next performed a more detailed steady-state kinetic analysis of the Sir2Tm enzyme's ability to deacetylate the K382azaKAc-containing peptide (Figure 5). We observed that Sir2Tm shows a significantly lower K_m of 10.9 ± 4.8 versus $71.8 \pm 24.5 \mu\text{M}$ for natural substrate. The catalytic efficiencies (k_{cat}/K_m) for the azaKAc and K382KAc peptides are similar (within 2-fold), suggesting that the acetyl-azalysine substrate leads to a more stable Michaelis complex.

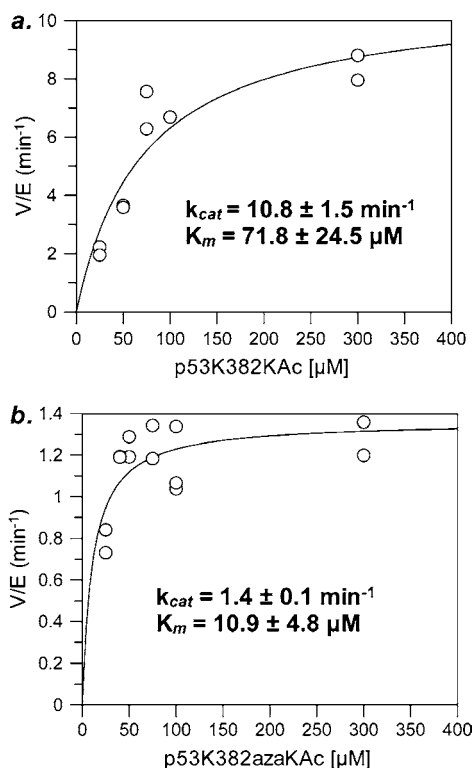


Figure 5. Comparison of rate and binding constants for Sir2Tm deacetylation reactions with p53 (372–389) peptides containing (a) acetyl-lysine (K382KAc) or (b) acetyl-azalysine (K382azaKAc) at 0.5 mM NAD.

Detection of an Acetyl-Azalysine ADP-Ribose Adduct.

We hypothesized that the alternate substrate, K382azaKAc, might generate a stabilized enzyme-catalyzed intermediate, akin to the *S*-alkylimidate adduct formed with the thioacetyl-lysine substrate that was observed by Smith et al.⁴⁵ We thus analyzed the Sir2Tm/K382azaKAc reaction mixture using MALDI-TOF mass spectrometry and, as expected, observed substrate, as well as deacetylated product (Figure 6 and Supporting Information Figure S1). In addition, there was an extra peak with $m/z = 2658$ (Figure 6). This mass is 18 Da lower than calculated for the simple alkylimidate adduct, potentially reflecting loss of a water molecule (Supporting Information Figure S2). This $m/z = 2658$ adduct peak was also observed in a reaction in which

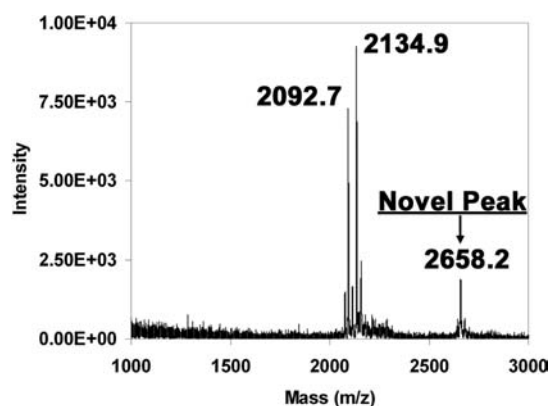


Figure 6. MALDI-TOF analysis of a Sir2Tm deacetylation reaction performed in the presence of K382azaKAc and Sir2Tm using positive ion linear mode.

human SIRT1 was used in place of Sir2Tm (Supporting Information Figure S3a). As a control, it was shown that Sir2Tm treatment of standard p53 peptide K382KAc did not result in a similar adduct (Supporting Information Figure S4c). Moreover, if enzyme or NAD were omitted, no peak with $m/z = 2658$ was observed (Supporting Information Figure S3[b-c]).

It was formally possible that the deacetylated product K382azaK could react with NAD or 2'-*O*-acetyl-ADP ribose. Mass spectrometric analysis of a K382KAc/Sir2Tm reaction spiked with K382azaK showed no evidence of the $m/z = 2658$ adduct (data not shown). Taken together, these data are consistent with the possibility that the adduct represents a derailed intermediate along the sirtuin deacetylation pathway.

Characterization of an Acetyl-Azalysine-ADP-Ribose Adduct. To further characterize the chemical nature of the $m/z = 2658$ adduct, we synthesized the ¹⁵N,¹⁵N,¹³C,¹³C-K382azaKAc labeled peptide in which the isotopes were introduced in the acetyl-hydrazide sites (Figure 2b and Supporting Information Figures S5 and S6). Labeled K382azaKAc was then subjected to Sir2Tm treatment in the presence of NAD. Mass spectrometry revealed the formation of an adduct related to the $m/z = 2658$ peak, but 4 mass units larger than the natural abundance compound (Supporting Information Figures S4a, S7, and S8). This result suggests that the $m/z = 2658$ adduct retains the acetyl-hydrazide atoms present in the peptide substrate.

To further investigate the structure of the $m/z = 2658$ adduct, we treated the K382azaKAc/Sir2Tm enzymatic reaction mixture with snake venom phosphodiesterase. Mass spectrometric analysis revealed the emergence of a peak corresponding to the $m/z = 2658$ adduct minus an AMP molecule (Supporting Information Figure S9). We confirmed the presence of both the ADP and AMP moieties by performing LC-MS/MS on the novel species (Supporting Information Figure S10). These data highly suggest that the peak of interest contains a significant portion of the NAD cofactor. In addition, tryptic digestion of the reaction mixture led to a truncated peptide that had a MW consistent with ADP-ribose attachment through the acetyl-azalysine moiety (Supporting Information Figure S11), and not some distal residue, as could be possible for ADP-ribosylation reactions sometimes proposed for sirtuins.^{57–59}

To further characterize the nature of the $m/z = 2658$ adduct, we employed a biotinylated version of NAD, 6-biotin-17-NAD (biotin-NAD), that can be turned over by sirtuins as an NAD alternate substrate (Supporting Information Figure S12), and that we hypothesized could be used in Western blots to assess adduct formation. In fact, treatment of K382azaKAc with Sir2Tm or SIRT1 and biotin-NAD generated a positive signal when probed with streptavidin-horse radish peroxidase (HRP) (Figure 7a; lanes 7 and 8). This signal appeared in a time-dependent fashion (Figure 7b), was dependent on each component of the reaction (Figure 7a; lanes 4–6), and was not detected with nonbiotinylated NAD, K382KAc, or deacetylated K382azaK (Figure 7a; lanes 1–3). We were also able to use biotin-NAD and a standard, biotinylated peptide to estimate how much of the $m/z = 2658$ adduct was being formed during the course of a typical reaction (Figure 7c and Supporting Information Figure S13). In this experiment, we found that after 60 min, about 2.5% ($5.1 \pm 2.1 \mu\text{M}$) of total substrate had been converted to the peptide-cofactor adduct. While slow relative to the natural deacetylation reaction, K382azaKAc-NAD adduct formation is much more rapid than

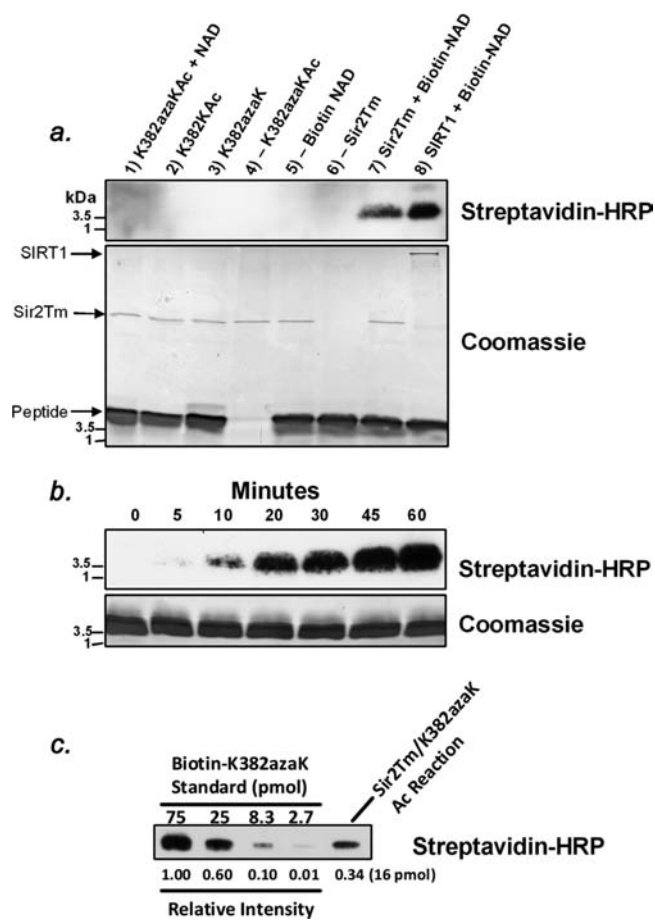


Figure 7. (a) Western blot analysis of 60 min sirtuin reactions with variations in reaction components. (b) Western blot analysis of time-dependent formation of novel sirtuin adduct. (c) Representative Western blot analysis using standard concentrations of a biotinylated-p53(372–389)K382azaK peptide to quantitate 16 pmol of adduct formation. An average of four 60 min experiments resulted in a final adduct concentration of $\sim 5 \mu\text{M}$ or 2.5% conversion from starting material.

rates reported for conventional ADP ribosylation by a sirtuin,⁵⁹ consistent with the idea that these are different chemical reactions. Interestingly, neither the Sir2Tm nor SIRT1 deacetylation reaction of natural acetyl-lysine peptide is potentially inhibited by K382azaKAc peptide (Supporting Information Figures S14 and S15), consistent with the fact the adduct is not formed in large quantity.

On the basis of the cumulative evidence and the expected chemical reactivity of the putative intermediate, we propose that the structure of the adduct is as shown in Figure 8b, structure 18. Because our data support the addition of an ADP-ribose moiety to our K382azaK peptide, we sought a more direct means of confirming the novel C1'–N bond formation (17) between the ribose moiety and the ϵ -nitrogen of the azaKAc side-chain in the proposed oxadiazine ring in structure 18. To validate the presence of the C1'–N bond in the $m/z = 2658$ adduct, we employed the ^{15}N , ^{15}N , ^{13}C , ^{13}C –K382azaKAc labeled peptide and Sir2Tm to generate a sufficiently large quantity of adduct that could be purified using ion-exchange chromatography (Supporting Information Figure S16).

Following ion-exchange chromatography, ^1H – ^{15}N HSQC spectra of the concentrated fractions revealed the presence of a novel ^1H signal at around 5.1 ppm (Figure 9 and Supporting

Information Figure S17) that is in the approximate range of reported ribose O–CH–N protons,⁶⁰ and that is not found in the unreacted ^{15}N , ^{15}N , ^{13}C , ^{13}C –K382azaKAc starting material (Supporting Information Figure S18). This signal confirms the formation of an N–C bond between the ribose C1' and the ϵ -nitrogen of the azaKAc side chain as depicted in structure 18. ^1H – ^{13}C – ^{13}C COSY spectra also show an upfield shift in the ^{13}C signal for the acetyl group carbonyl carbon in the purified adduct (Supporting Information Figure S19) compared with the starting material (Supporting Information Figure S20), consistent with an amide to imidate transformation.⁶¹ Taken together with the above mass spectrometric and biochemical experiments, we believe that the above NMR structural data convincingly establish the structure of the peptide–cofactor adduct as the oxadiazine (18).

LSD1 Inhibition by H3K4azaK. As previously mentioned, a one-carbon extended structural analogue of azalysine, in the context of a histone H3 tail peptide at position 4 (Figure 10a), is a potent suicide inactivator of LSD1.⁶² To explore the potential of H3K4azaK itself as an LSD1 inhibitor, we synthesized the requisite peptide (Figure 10b) and examined its properties with the demethylase. These experiments showed that H3K4azaK is a potent time-dependent inhibitor of LSD1, comparable to hydrazino-Lys4 H3-21 (Figure 10c). Interestingly, we found that the p53(372–389)K382azaK peptide exhibits considerably weaker inhibition, demonstrating the importance of peptide sequence context in the inactivation (Supporting Information Figure S21).

A proposed mechanism for hydrazine inactivation of amine oxidase enzymes involves oxidation of the hydrazine to the diazonium species, followed by nucleophilic attack of FADH to generate a covalent adduct.⁵⁰ Consistent with such a model, mass spectrometric analysis of the reaction mixture of LSD1 with H3K4azaK gave rise to a peak with molecular weight of the predicted peptide–flavin conjugate (Supporting Information Figure S22). These data corroborate the kinetic studies that H3K4azaK is a suicide inhibitor of LSD1.

DISCUSSION

While the sirtuin reaction (Figure 8a) has long been proposed to involve a mechanism in which the 2'-hydroxy group of the ADP ribose attacks the imidate intermediate (10), no direct observation of the resulting bicyclic species (11) has been reported.³⁷ The $m/z = 2658$ adduct formed by reaction of K382azaKAc with sirtuin is novel evidence for the possibility that the enzymatic mechanism (Figure 8b) proceeds through 2'-hydroxy attack on a peptide-imidate-glycoside species (14 to 15), followed by a series of rearrangement reactions (16 to 17) to form the oxadiazine (18). The proposed chemical structure of the final adduct (18) is supported by chemical plausibility, as well as by the NMR spectroscopy studies, mass spectrometric data, isotope labeling experiments, phosphodiesterase experiments, and biotin tagging. It is interesting that the hydrazine group apparently allows for progression beyond the imidate intermediate trapped when thioacetyl-lysine is processed by sirtuins.⁴⁴ It corroborates the observation that the oxyimide intermediate is more susceptible to attack than the thioimide in the corresponding thioacetyl-lysine reaction.

The resistance of K382azaKAc to HDAC8 deacetylation relative to sirtuin processing is inverse with respect to the properties of the thioacetyl-Lys peptide. One can surmise that the hydrazido functionality may interfere with metal coordina-

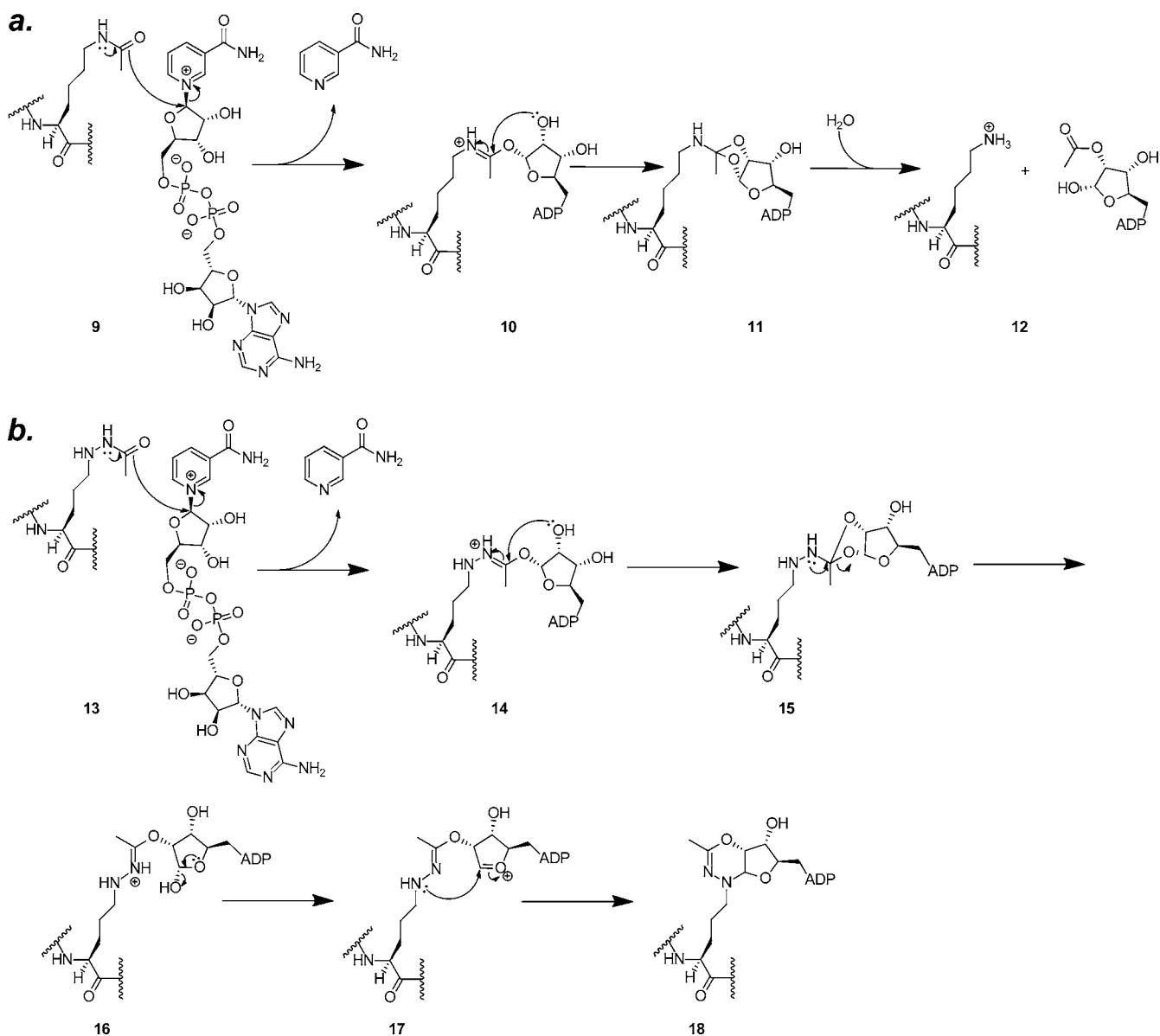


Figure 8. (a) Proposed mechanism by which sirtuins are thought to deacetylate an acetyl-lysine residue. (b) Proposed mechanism to account for the formation of a novel azaKAc-ADP-ribose adduct (18).

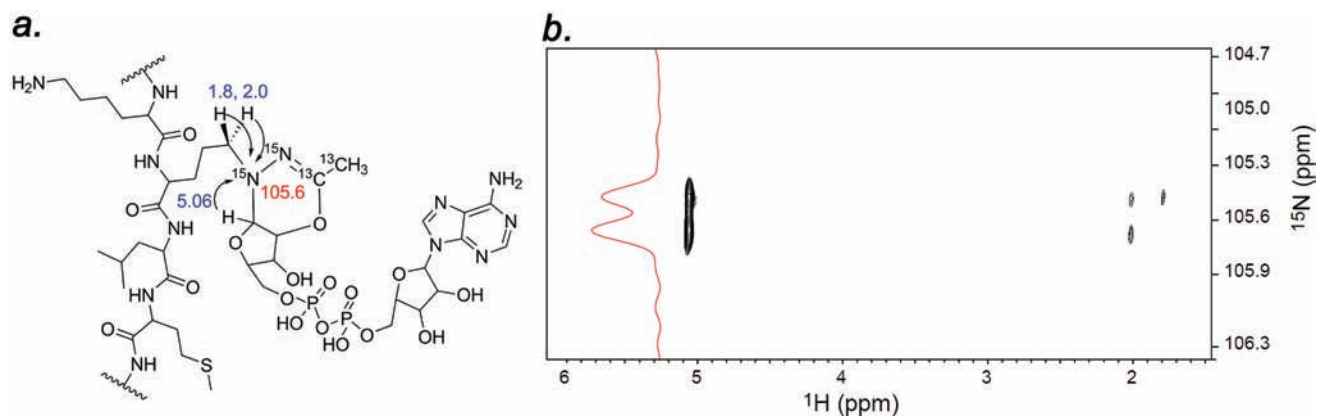


Figure 9. (a) Chemical schematic showing correlations of the C1' proton of the ribose ring and δ -methylene protons of the azaKAc side chain with the ϵ -nitrogen of the azaKAc side chain. Chemical shifts for the protons are presented in blue and the nitrogen chemical shift is shown in red. (b) Region of a ^1H - ^{15}N long-range gHSQC NMR spectrum acquired at 600 MHz (^1H) and 30 °C. The splitting along the ^{15}N dimension, as shown in the cross section parallel to the ^{15}N axis, corresponds to a $^1J_{\text{NN}} \sim 13$ Hz.

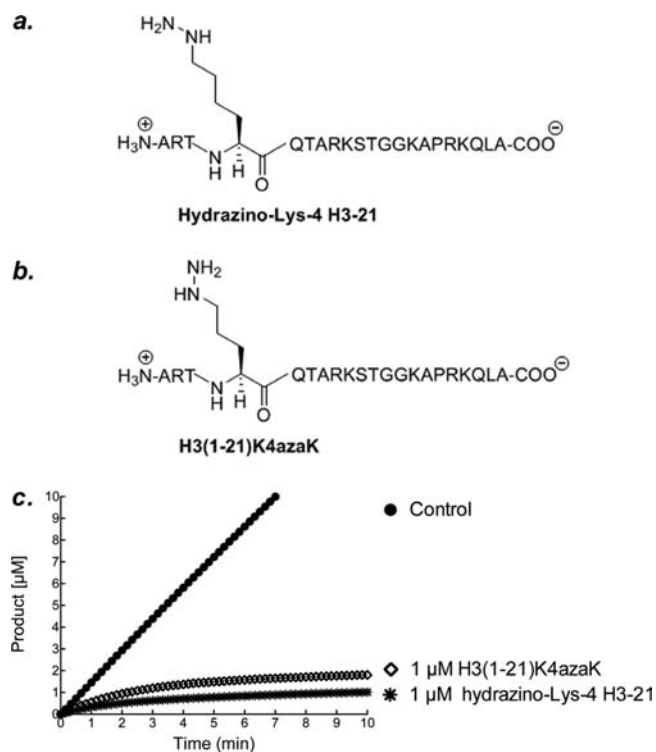


Figure 10. Structures of LSD1 inhibitors: (a) hydrazino-Lys-4 H3-21, and (b) H3(1–21)K4azaK. (c) Steady-state progress curves obtained for the inactivation of GST-LSD1 in the presence of 1 μM hydrazino-Lys-4 H3-21 or H3(1–21)K4azaK.

tion or otherwise distort the leaving group geometry of the acetyl group. Such orthogonality to thioacetyl-Lys may allow for biochemical applications to dissect the role of specific deacetylases in protein acetylation reversal. In future work, it will be interesting to explore this functionality and its interaction with other deacetylases not yet explored.

The finding that the H3K4azaK peptide is a potent suicide inhibitor of LSD1 extends the application of this unnatural amino acid to another epigenetic modifying enzyme. The use of the azalysine building block for peptide synthesis provides greater versatility relative to the prior effort where the homologous hydrazino-Lys derivative was introduced post-peptide assembly.⁵⁰ Given prior LSD1 work on the hydrazino-Lys analogue, these findings point to some plasticity in the tolerance of this enzyme to alterations in the peptide side chain. It will be interesting in future studies to optimize the chemical context of the hydrazine group to improve the pharmacologic properties of this probe. The current peptide sequence of the H3(1–21)K4azaK inhibitor would likely be unable to penetrate cell membranes, and would be unstable due to proteolytic clearance. Although hydrazine functionalities may have some limitations due to hepatic metabolism,⁶³ we note that phenethylhydrazine is a well-established inhibitor of monoamine oxidases used in the treatment of clinical depression.^{64,65} These data provide impetus for the development of new hydrazine-containing LSD1 inhibitors with clinical potential.^{66–72}

METHODS AND MATERIALS

General. All chemicals were purchased from Sigma-Aldrich (St. Louis, MO) unless otherwise specified. NMR spectra were obtained on a Varian 400 MHz spectrometer unless otherwise specified.

Accurate mass ESI spectra were obtained using the High Resolution Mass Spectrometry Facility at the University of California, Riverside.

Synthesis. *2-Dibenzylamino-5-oxo-pentanoic Acid Benzyl Ester (4)*. This compound was prepared as described previously.⁵²

2-Dibenzylamino-5-acetylhydrazono-pentanoic Acid Benzyl Ester (5a). The protected aldehyde (**4**) (500 mg, 1.2 mmol) was dissolved in anhydrous THF (4 mL) and added to a 25 mL round-bottom flask. Acetic hydrazide (109 mg, 1.32 mmol) was added to the flask and the contents were magnetically stirred under N_2 for 48 h at room temperature (rt). The crude reaction mixture was subjected to flash column chromatography (50–60% ether/petroleum ether) on silica gel (200–400 mesh; mean pore diameter 60 Å). Fractions containing the desired compound were concentrated in vacuo and pure compound **5a** was obtained as a slightly yellow foam (330 mg, 60% yield). ^1H NMR (400 MHz, CDCl_3): δ = 1.92–1.97 (m, 2H), 2.07 (s, 3H), 2.18–2.27 (m, 1H), 2.31–2.40 (m, 1H), 3.45 (m, J = 7.3 Hz, 1H), 3.68 (AB system, J = 13.7 Hz, 4H), 5.20 (AB system, J = 12.2 Hz, 2H), 6.90 (t, J = 4.6 Hz, 1H), 7.18–7.41 (m, 15H), 9.42 (s, 1H). ^{13}C NMR (100 MHz, CDCl_3): δ = 20.28, 25.61, 28.52, 54.53, 59.59, 66.22, 127.22, 128.41, 128.52, 128.58, 128.74, 129.00, 136.08, 139.38, 146.65, 172.56, 173.96. HRMS calcd $[\text{M} + \text{H}]^+$: 458.2438; found, 458.2445.

2-Dibenzylamino-5-acetylhydrazine-pentanoic Acid Benzyl Ester (6a). Using a procedure inspired by the reduction of enediamines,⁵⁵ the hydrazone (**5a**) (490 mg, 1.1 mmol) was dissolved in anhydrous ethanol (5 mL) and transferred to a 25 mL round-bottom flask. To this mixture, acetic acid (378 μL , 6.6 mmol) was added and allowed to magnetically stir for about 5 min. Sodium cyanoborohydride (276 mg, 4.4 mmol) was then added, and the solution initially effervesced and then turned a transparent yellow color. A rubber septum with a needle inserted for venting was placed on the flask and the reaction was allowed to proceed overnight under magnetic stirring at rt. The reaction contents were directly concentrated onto silica gel; a workup with extraction into ethyl acetate, followed by washes with brine, and then dried over magnesium sulfate could also be employed prior to column purification. Compound **6a** was separated by flash column chromatography (0–2% methanol/methylene chloride + 1% NH_4OH) on silica gel (200–400 mesh; mean pore diameter 60 Å). Fractions containing compound **6a** were concentrated to yield a slightly yellow foam (154 mg, 31% yield) that was sufficiently pure for further use. ^1H NMR (400 MHz, CDCl_3): small rotamers observed but not reported. δ = 1.32–1.42 (m, 1H), 1.57–1.68 (m, 1H), 1.78–1.84 (m with overlap, 2H), 1.89 (s with overlap, 3H), 2.69 (m, 2H), 3.38 (t, J = 7.5 Hz, 1H), 3.72 (AB system, J = 13.9 Hz, 4H), 5.23 (AB system, J = 12.2 Hz, 2H), 7.23–7.44 (m, 15H). ^{13}C NMR (100 MHz, CDCl_3): small rotamers observed but not reported. δ = 21.25, 24.41, 26.86, 51.43, 54.54, 60.66, 66.20, 127.15, 128.41, 128.51, 128.63, 128.75, 128.92, 136.12, 139.58, 169.76, 172.92. HRMS calcd $[\text{M} + \text{H}]^+$: 460.2595; found, 460.2589.

*2-Dibenzylamino-5-acetylhydrazine(*t*-butyl carbamate)-pentanoic Acid Benzyl Ester (7a)*. Compound **6a** (154 mg, 0.34 mmol) was dissolved in dichloromethane (3 mL) in a 50 mL round-bottom flask. Di-*tert*-butyl dicarbonate (98 mg, 0.45 mmol) and one crystal of 4-dimethylaminopyridine were then added to the reaction mixture. The reaction was allowed to proceed at rt with magnetic stirring for 70 min or until completion was observed using TLC. The reaction contents were concentrated onto silica gel and compound **7a** was separated by flash column chromatography (0–40% ethyl acetate/hexanes) on silica gel (200–400 mesh; mean pore diameter 60 Å). Fractions containing compound **7a** were concentrated to obtain an extremely viscous clear oil (113 mg, 59% yield) that was sufficiently pure for further use. ^1H NMR (400 MHz, CDCl_3): small rotamers observed but not reported. δ = 1.37–1.4 (s with rotamer, 10H), 1.61–1.78 (m, 3H), 1.88 (s, 3H), 3.32–3.35 (m, 3H), 3.69 (AB system, J = 13.9 Hz, 4H), 5.19 (AB system, J = 12.2 Hz, 2H), 7.21–7.40 (m, 15H). ^{13}C NMR (100 MHz, CDCl_3): small rotamers observed but not reported. δ = 20.90, 24.32, 26.54, 28.28, 49.73, 54.63, 60.63, 66.26, 82.19, 127.20, 128.45, 128.56, 128.67, 128.78, 128.88, 136.10, 139.58,

155.26, 169.53, 172.96. HRMS calcd $[M + H]^+$: 560.3119; found, 560.3128.

2-Fluorenylmethoxycarbamate-5-acetylhydrazine(*t*-butyl carbamate)-pentanoic Acid (8a). Removal of the benzyl protecting groups from compound **7a** was accomplished using catalytic transfer hydrogenation.⁵⁶ Formic acid (4.4%) in methanol was chilled on dry ice in a 50 mL Falcon tube 10 min prior to initiating the reaction. A 25 mL round-bottom flask containing compound **7a** (113 mg, 0.2 mmol) was also chilled on dry ice, evacuated, and purged with N₂. Formic acid (4.4%) in methanol (10 mL) was added to the chilled reaction vessel. The resulting solution was magnetically stirred for 5 min on dry ice, and a roughly stoichiometric amount of palladium black (120 mg, high surface area, 99.8%) was cautiously and slowly added to avoid fulmination. The dry ice was removed and the reaction was allowed to proceed overnight at rt under magnetic stirring and N₂ after which the reaction appeared complete by TLC. The palladium was filtered off and the resulting methanol solution was concentrated in vacuo. Water (~5 mL) was then added to the flask followed by dichloromethane (~5 mL), and the aqueous layer was extracted and concentrated, resulting in a faintly yellow crystalline film. This debenzylated amino acid (57 mg) was sufficiently pure to be taken forward without further purification. ¹H NMR (400 MHz, CD₃OD): δ = 1.44–1.48 (s with rotamer, 9H), 1.60–1.77 (m, 2H), 1.85–2.05 (m with overlap, 2H), 1.96 (s with overlap, 3H), 3.44–3.52 (m, 2H), 3.89 (t, *J* = 6.4 Hz, 1H). ¹³C NMR (100 MHz, CD₃OD): δ = 20.70, 24.57, 28.58, 29.12, 54.34, 82.65, 156.72, 172.64. HRMS calcd $[M + H]^+$: 290.1710; found, 290.1716.

Water (2 mL), 1,4-dioxane (5 mL), and potassium carbonate (41 mg, 0.3 mmol) were added to a 50 mL round-bottom flask and magnetically stirred for 5 min in an ice-bath at 0 °C. To this solution, the deprotected amino acid from the previous step was added, and this mixture was allowed to stir for approximately 5 min. 9-Fluorenylmethyl succinimidyl carbonate (84 mg, 0.25 mmol) was then added to the reaction mixture and magnetically stirred for 2.5 h at 0 °C. The reaction was then moved to rt and allowed to react for an additional 30 min prior to concentration. The mixture was then extracted into ethyl acetate (10 mL) and washed with 10% citric acid in water (10 mL), and the organic layer dried over magnesium sulfate, filtered, and concentrated. Compound **8a** was then purified by preparative reverse-phase HPLC (acetonitrile/water/0.05% formic acid, Varian Dynamax 250 × 21 mm C18 Microsorb column). Fractions containing compound **8a** were combined and concentrated, yielding a white solid (66.3 mg, 65% yield from compound **7a**). ¹H NMR (400 MHz, CDCl₃): δ = 1.43–1.44 (s with rotamer and overlap, 9H), 1.61–1.69 (m with overlap, 2 H), 1.69–1.78 (m with overlap, 1 H), 1.95–1.99 (s with rotamer, 4H), 3.46–3.54 (m, 2H), 4.18 (t, *J* = 6.9 Hz, 1H), 4.34 (d with overlap, *J* = 7.0 Hz), 4.44 (m with overlap, 1H), 5.86–6.06 (br, –NH) 7.24–7.28 (m, 2H), 7.36 (t, *J* = 7.4 Hz, 2H), 7.53–7.60 (m, 2H), 7.72 (d, *J* = 7.5 Hz, 2H). ¹³C NMR (100 MHz, CDCl₃): small rotamers observed but not reported δ = 20.86, 23.54, 28.35, 29.52, 47.29, 49.51, 53.68, 67.34, 82.85, 120.17, 125.32, 127.26, 127.93, 141.46, 143.84, 156.29, 156.73, 170.57, 175.56. HRMS calcd $[M + Na]^+$: 534.2216; found, 534.2202.

2-Dibenzylamino-5-hydrazine(*t*-butyl carbamate)-pentanoic Acid Benzyl Ester (5b). The protected aldehyde (**4**) (378 mg, 0.94 mmol) was dissolved in anhydrous THF (5 mL) and added to a 50 mL round-bottom flask. *t*-Butyl carbamate (162 mg, 1.2 mmol) was added to the flask and the contents were magnetically stirred under N₂ for 12 h at rt. The reaction contents were concentrated onto silica gel and compound **5b** was separated by flash chromatography (0–15% ethyl acetate/hexanes) on silica gel (200–400 mesh; mean pore diameter 60 Å). Fractions containing compound **5b** were concentrated in vacuo, affording a slightly yellow foam (257 mg, 53% yield) that was sufficiently pure for further use. ¹H NMR (400 MHz, CDCl₃): small rotamers observed but not reported δ = 1.52–1.57 (s with rotamer, 9H), 1.94–2.06 (m, 2H), 2.19–2.26 (m, 1H), 2.44–2.47 (m, 1H), 3.44 (t, *J* = 7.2 Hz), 3.74 (AB system, *J* = 13.7 Hz, 4H), 5.24 (AB system, *J* = 12.1 Hz, 2H), 6.88 (s, 1H), 7.25–7.44 (m, 15H), 7.86 (br, –NH). ¹³C NMR (100 MHz, CDCl₃): rotamers observed but not reported δ = 23.21, 26.17, 28.25, 54.33, 59.87, 66.06, 80.70, 127.01,

128.25, 128.31, 128.46, 128.54, 128.86, 135.90, 139.17, 146.21, 152.52, 172.18. HRMS calcd $[M + H]^+$: 516.2857; found, 516.2857.

2-Dibenzylamino-5-hydrazine(*t*-butyl carbamate)-pentanoic Acid Benzyl Ester (6b). The hydrazone (**5b**) (257 mg, 0.5 mmol) was dissolved in anhydrous ethanol (6 mL) and transferred to a 25 mL round-bottom flask. To this flask, acetic acid (172 μ L, 3 mmol) was added and allowed to magnetically stir for about 5 min. Sodium cyanoborohydride (126 mg, 2 mmol) was then added. The solution initially effervesced and the solution turned a transparent yellow color. A rubber septum with a needle inserted for venting was placed on the flask and the reaction was allowed to proceed overnight under magnetic stirring at rt. The next morning, the reaction contents were diluted with ethyl acetate (10 mL) and the organic layer was extracted by washing with aqueous, saturated sodium bicarbonate (3 × 10 mL) followed by brine (2 × 10 mL). The organic layer was then concentrated directly onto silica gel (200–400 mesh; mean pore diameter 60 Å) and compound **6b** was separated by flash chromatography (0–15% ethyl acetate/hexanes). Fractions containing compound **6b** were concentrated in vacuo to yield an extremely viscous clear oil (167 mg, 65% yield). ¹H NMR (400 MHz, CDCl₃): δ = 1.37–1.54 (m with overlap, 1H), 1.50 (s with overlap, 9 H), 1.61–1.72 (m, 1 H), 1.80–1.91 (m, 2H), 2.74 (t, *J* = 6.8 Hz, 2 H), 3.41 (t, *J* = 7.5 Hz, 1H), 3.76 (AB system, *J* = 13.8 Hz, 4 H), 5.25 (AB system, *J* = 12.2 Hz, 2 H), 6.22 (br, –NH), 7.24–7.48 (m, 15 H). ¹³C NMR (100 MHz, CDCl₃): δ = 24.41, 26.95, 28.44, 51.51, 54.48, 60.63, 66.02, 80.32, 127.05, 128.32, 128.38, 128.56, 128.65, 128.88, 136.14, 139.57, 156.80, 172.74. HRMS calcd $[M + H]^+$: 518.3013; found, 518.3008.

2-Dibenzylamino-5-hydrazine(*t*-butyl carbamate)₂-pentanoic Acid Benzyl Ester (7b). Compound **6b** (167 mg, 0.32 mmol) was dissolved in dichloromethane (3 mL) in a 100 mL round-bottom flask. Di-*tert*-butyl dicarbonate (83 mg, 0.38 mmol) and one crystal of 4-dimethylaminopyridine were then added to the reaction mixture. The reaction was allowed to proceed at rt with magnetic stirring for 3.5 h. The reaction contents were concentrated onto silica gel and compound **7b** was separated by flash chromatography (0–15% ethyl acetate/hexanes) on silica gel (200–400 mesh; mean pore diameter 60 Å). Fractions containing compound **7b** were concentrated in vacuo to yield compound **7b** as an extremely viscous clear oil (143 mg, 72% yield) that was sufficiently pure for further use. ¹H NMR (400 MHz, CDCl₃): small rotamers observed but not reported δ = 1.38–1.57 (m with overlap, 1H), 1.54 (s with overlap, 18 H), 1.66–1.93 (m, 3H), 2.75 (t, *J* = 7 Hz, 2H), 3.41 (t, *J* = 7.5 Hz, 1H), 3.74 (AB system, *J* = 13.8 Hz, 4H), 5.23 (AB system, *J* = 12.2 Hz, 2 H), 7.23–7.47 (m, 15 H). ¹³C NMR (100 MHz, CDCl₃): small rotamers observed but not reported δ = 24.49, 27.10, 28.12, 50.88, 54.44, 60.68, 66.00, 83.09, 127.03, 128.31, 128.53, 128.63, 128.86, 136.11, 139.49, 152.36, 172.64. HRMS calcd $[M + H]^+$: 618.3538; found, 618.3536.

2-Fluorenylmethoxycarbamate-5-hydrazine(*t*-butyl carbamate)₂-pentanoic Acid (8b). Complete removal of the benzyl protecting groups from compound **7b** was accomplished using catalytic transfer hydrogenation.⁵⁶ Formic acid (4.4%) in methanol was chilled on dry ice in a 50 mL Falcon tube 10 min prior to initiating the reaction. A 100 mL round-bottom flask containing compound **7b** (143 mg, 0.23 mmol) was also chilled on dry ice, evacuated, and purged with N₂. Formic acid (4.4%) in methanol (10 mL) was added to the chilled reaction vessel. The resulting solution was magnetically stirred for 5 min on dry ice. A roughly stoichiometric amount of palladium black (143 mg, high surface area, 99.8%) was cautiously and slowly added to avoid fulmination. This dry ice was removed and the reaction was allowed to proceed overnight at rt under magnetic stirring and N₂, after which the reaction appeared to be complete by TLC. The palladium was filtered off and the resulting methanol solution was concentrated in vacuo. Water (~5 mL) was then added to the flask, followed by dichloromethane (~5 mL), and the aqueous layer was extracted and concentrated, resulting in a white crystalline film (78 mg). This material was taken forward without further purification. ¹H NMR and ¹³C NMR contain some impurities. HRMS calcd $[M + H]^+$: 348.2129; found, 348.2129

Water (2 mL), 1,4-dioxane (5 mL), and potassium carbonate (46 mg, 0.33 mmol) were added to a 50 mL round-bottom flask and magnetically stirred for 5 min in an ice-bath at 0 °C. To this solution, the deprotected amino acid from the previous step, assumed to be pure for the purpose of calculations (78 mg, 0.22 mmol), was added and this mixture was allowed to stir for approximately 5 min. 9-Fluorenylmethyl succinimidyl carbonate (94 mg, 0.28 mmol) was then added to the reaction mixture and magnetically stirred for 1.5 h at 0 °C. The reaction was then moved to rt and allowed to react for an additional 60 min prior to concentration. The mixture was then extracted into ethyl acetate (10 mL) and washed with 10% citric acid in water (10 mL), and the organic layer dried over magnesium sulfate, filtered, and concentrated in vacuo. Compound **8b** was then purified by preparative reverse-phase HPLC (acetonitrile/water/0.05% formic acid, Varian Dynamax 250 × 21 mm C18 Microsorb column). Fractions containing compound **8b** were combined and concentrated, yielding a white solid (28 mg, 21% yield from compound **7b**). ¹H NMR (400 MHz, CDCl₃): δ = 1.45–1.67 (s with overlap, 20 H), 1.86–2.01 (m, 2H), 2.88 (t, *J* = 6.3 Hz, 2H), 4.21 (t, *J* = 7 Hz, 1H), 4.32–4.48 (m, 3 H), 5.86 (d, *J* = 7.2 Hz, 1H), 6.10 (br, –NH), 7.28–7.32 (m, 2H), 7.36–7.40 (m, 2H), 7.59–7.61 (m, 2H), 7.75 (d, *J* = 7.5 Hz, 2H). ¹³C NMR (100 MHz, CDCl₃): small rotamers observed but not reported δ = 23.18, 28.25, 30.02, 47.34, 50.69, 53.89, 67.31, 84.19, 120.12, 125.39, 127.28, 127.86, 141.46, 143.99, 152.31, 156.37, 175.11. HRMS calcd [M + H]⁺: 570.2810; found, 570.2803.

Peptide Synthesis. Peptides were synthesized using standard Fmoc-solid phase peptide chemistry on a PS3 Peptide Synthesizer (Protein Technologies, Tucson, AZ). All unnatural amino acids were manually coupled to the nascent peptide at a ratio of 1.5 equiv of amino acid to peptide resin. The coupled peptide was then returned to the synthesizer for completion of the synthesis. Peptides were cleaved with Reagent K and subsequently purified using a Varian Dynamax Microsorb C18 preparative column (Agilent, Santa Clara, CA). Purified peptide was lyophilized and its mass confirmed with an Applied Biosystems Voyager DE-STR MALDI-TOF mass spectrometer (Life Technologies, Carlsbad, CA).

Peptide purity was confirmed by amino acid analysis using the services offered by the W. M. Keck Biotechnology Resource Laboratory at Yale University (New Haven, CT).

Protein Purification. Sir2Tm, inserted in the pET11a plasmid, was generously provided by the Wolberger laboratory. We expressed and purified Sir2Tm as inclusion bodies as was previously described by Smith et al.⁷³ The enzyme was estimated to be about 90% pure by Coomassie-stained SDS–PAGE. This material was used for assay experiments after dialyzing away the urea in the resolubilization buffer.

SIRT1 and HDAC8 were both purchased from Enzo Life Sciences (Farmingdale, NY). LSD1 was expressed and purified as was previously described.⁵⁰

HPLC Deacetylation Assays. Sirtuin and HDAC8 deacetylase assays were essentially performed as was previously described.³⁸ All time points were performed in at least duplicate. Areas under the curve for separated peptides were integrated using the Varian Workstation Integrative Graphics software, from which rate values could be determined.

HDAC8 Deacetylation Assay. A typical HDAC8 deacetylation reaction was performed as follows: a 200 μL reaction mixture containing 1× metal buffer (25 mM Tris-Cl, pH 8.0, 137 mM NaCl, 2.7 mM KCl, and 1 mM MgCl₂) and peptide (0–500 μM) was initiated at 37 °C by addition of enzyme (3.5 μM HDAC8 (18 U) final). Aliquots of 50 μL were taken at 0, 5, 10, and 20 min time points and quenched with 50 μL of HDAC8 arresting buffer (1 M HCl, 0.16 M acetic acid). Ten microliters of 8 M urea was then added to help solubilize any precipitated peptide and the mixture was centrifuged in an Amicon Ultra 0.5 mL 10 000 MWCO filter unit (Millipore, Billerica, MA) at 14 000g for 10 min. The resulting filtrate was then injected onto a Varian Microsorb C18 analytical column (Agilent, Santa Clara, CA). The p53(372–389)K382KAc and p53(372–389) peptides were separated using a reverse phase system where solvent A = (H₂O + 0.05% trifluoroacetic acid) and solvent B = (acetonitrile +

0.05% trifluoroacetic acid): linear increase from 5% Solvent B to 25% Solvent B over the course of 50 min.

To separate the p53(372–389)K382azaKAc from the p53(372–389)K382azaK peptide, we employed a high resolution Varian Pursuit XRs analytical C18 Column (A6001250X046; Agilent, Santa Clara, CA). These peptides were separated using the same solvent system above, but with a different program: linear increase from 0% Solvent B to 19% Solvent B over the course of 80 min.

Sirtuin Deacetylation Assay. A typical sirtuin deacetylation assay was performed as follows: a 200 μL reaction mixture containing: 1× metal buffer, 500 μM NAD, and peptide (0–500 μM) was initiated by addition of enzyme (0.3–0.15 μM Sir2Tm or 0.07 μM (1U) SIRT1) at 37 °C. Aliquots of 50 μL were taken at 0, 5, 10, and 20 min time points and quenched with 50 μL of Sir2Tm arresting buffer (0.1 M HCl, 0.16 M acetic acid). Ten microliters of 8 M urea was then added and the mixture was centrifuged in an Amicon Ultra 0.5 mL 10 000 MWCO filter unit (Millipore, Billerica, MA) at 14 000g for 10 min. The resulting filtrate was then injected onto a Varian Microsorb C18 analytical column for the separation of the p53(372–389)K382KAc from the p53(372–389) peptide with the same solvent system as that used for HDAC8 above. The p53(372–389)K382azaKAc peptide was separated from the p53(372–389)K382azaK peptide using the Varian Pursuit XRs analytical C18 column as described above.

Mass Spectrometry. Samples were analyzed on an Applied Biosystems Voyager DE-STR MALDI-TOF mass spectrometer (Life Technologies, Carlsbad, CA). The spectrometer was calibrated using a Peptide Calibration Standard (222570; Bruker Daltonics, Billerica, MA). Samples were spotted onto 2,5-dihydroxybenzoic acid (DHB) matrix and analyzed by using either positive ion linear or reflection modes.

For mass spectrometric analysis of the sirtuin reactions, a 50 μL reaction volume containing 200 μM peptide, 200 μM NAD, and metal buffer was initiated with the addition of 20 μM Sir2Tm or 0.5 μM SIRT1. Individual reagents were omitted, and peptides varied, depending on the particular experiment. The reaction was allowed to proceed at 37 °C for 10 min. Ten microliters of reaction mixture was then desalted using a C18 Zip-Tip (Millipore, Billerica, MA) following the manufacturer's instructions. These reaction aliquots were then analyzed using MALDI-TOF.

Western Blot Analysis. For the reagent panel experiment (Figure 7a), a 27 μL reaction volume containing 200 μM K382azaKAc peptide, 200 μM biotin-NAD (BLG-N012–001; Axxora, San Diego, CA), and metal buffer was initiated with the addition of 0.6 μM Sir2Tm (lane 7) or SIRT1 (lane 8). Reaction components from a Sir2Tm reaction were omitted to account for the different conditions found in lanes 4–6. Sir2Tm assays containing nonbiotinylated NAD (200 μM) or different peptide substrates were also analyzed (lanes 1–3). Reactions were incubated at 37 °C for 60 min and then frozen in liquid N₂ prior to Western analysis.

For the time course study (Figure 7b), a 185 μL reaction volume containing 200 μM K382azaKAc, 200 μM biotin-NAD (BLG-N012–001, Axxora, San Diego, CA), and metal buffer was initiated with the addition of 0.6 μM Sir2Tm. Twenty-five microliters aliquots were taken by freezing them in liquid N₂ at 0, 5, 10, 20, 30, 45, and 60 min.

For the standard curve analysis (Figure 7c and Supporting Information Figure S13), a 27 μL reaction volume containing 200 μM peptide, 200 μM NAD or biotin-NAD (BLG-N012–001; Axxora, San Diego, CA), and metal buffer was initiated with the addition of 0.6 μM Sir2Tm. Reactions were incubated at 37 °C for 60 min and then frozen in liquid N₂ prior to Western analysis. Standard peptide samples correspond to a Biotin-PEG (9 atom)-p53(372–389)K382azaK peptide. Known concentrations were loaded as denoted in the respective figures.

Electrophoresis and Peptide Labeling. SDS/PAGE was performed as previously described.^{74,75} Samples were separated on 15% acrylamide gels and stained with Coomassie blue (#161–0406; Bio-RAD, Hercules, CA) or transferred to 0.45 μm PVDF membranes. Membranes were blocked overnight at 4 °C with 5% milk dissolved in TBS (10 mM Tris, pH 7.5, and 154 mM NaCl) followed by incubation with streptavidin–HRP (1:5000; #S-911; Molecular Probes, Carlsbad,

CA) diluted in TBS-T (TBS + 0.05% Tween 20) and 1% milk for 1 h at rt. Biotinylated peptides were detected by ECL plus chemiluminescent reagent (#RPN2132; GE Healthcare, Waukesha, WI) following manufacturer's protocol and exposed to X-ray film.

For the standard curve analysis (Figure 7c and Supporting Information Figure S13), after development of the X-ray film, the film was digitally scanned and the resulting images were analyzed using the ImageQuant software (GE Healthcare, Waukesha, WI).

Adduct Isolation Using Ion-Exchange Chromatography. A 250 μL Sir2Tm deacetylation reaction containing 200 μM p53(372–389)K382¹⁵N, ¹⁵N, ¹³C, ¹³C-azaKAc, 1 mM NAD, and 1 \times metal buffer was initiated with the addition of Sir2Tm (0.6 μM final) and allowed to proceed for 60 min at 37 $^{\circ}\text{C}$, after which 750 μL of buffer A (20 mM triethylammonium bicarbonate, pH 7.68, 20% acetonitrile, in water) was added to the reaction and the mixture centrifuged at 16 000g for 5 min. The 1 mL solution was then injected onto a PolyCAT A column (#204CT0510, PolyLC, Columbia, MD) and the adduct purified using a linear gradient of buffer A/B, 0–50% buffer B (800 mM triethylammonium bicarbonate, pH 7.68, 20% acetonitrile, in water) over 25 min (Supporting Information Figure S16b). In the ion-exchange chromatogram, the peak eluting earlier than the unreacted starting material was confirmed to be enriched with adduct using MALDI-TOF after Zip-Tip treatment (Supporting Information Figure S16c,d). Positive fractions were pooled, concentrated in vacuo, and placed on a lyophilizer overnight.

After approximately 30 reactions had been pooled, the resulting concentrate was resuspended in H₂O and lyophilized in order to aid in the removal of any residual triethylammonium bicarbonate. After repeating this once more, the final material was taken forward for NMR analysis.

NMR Analysis of Purified Adduct. The total isolated adduct was resuspended in 300 μL of D₂O (DLM-4-100, Cambridge Isotope Laboratories, Andover, MA) and transferred to a Shigemi microtube (Allison Park, PA) for NMR analysis.

For the H–N long-range HSQC of the adduct, the appropriate delay for H \rightarrow N magnetization transfer was set to 100 ms ($\sim 1/(2J_{\text{NH}})$). Other data acquisition parameters were as follows: (a) 64 scans/FID, recycle delay of 1.2s; (b) spectral widths, 17 ppm (¹H), 10 ppm (¹⁵N); (c) complex data points, 605 (¹H), 188 (¹⁵N); (d) spectrometer carrier positions, 4.72 ppm (¹H), 107.53 ppm (¹⁵N). The ¹⁵N spectrometer frequency was carefully optimized from 1D versions of the experiment. Total data acquisition time was approximately 9 h.

LSD1 Inhibition Studies. These assays were essentially performed as previously described.⁵⁰ The peptide inhibitors, hydrazino-Lys-4 H3-21, H3(1–21)K4azaK, and p53(372–389)K382azaK were tested using one of two variants of a horseradish peroxidase coupled assay that monitors the production of hydrogen peroxide. The time course for all reactions were measured under aerobic conditions using a Beckman Coulter (Brea, CA) DU 600 spectrophotometer equipped with a thermostatted cell holder ($T = 25^{\circ}\text{C}$). The 100 μL reactions were initiated by addition of GST-LSD1 to the reaction mixture. Reactions that tested inhibitory potency of p53(372–389)K382azaK peptide contained 50 mM HEPES buffer (pH 7.5), 0.1 mM 4-aminoantipyrine, 1 mM 3,5-dichloro-2-hydroxybenzenesulfonic acid, 0.76 μM horseradish peroxidase (Worthington Biochemical Corporation, Lakewood, NJ), 300 μM substrate (H3(1-21)K4Kme2), 110 nM GST-LSD1. Absorbance changes were monitored at 515 nm, and an extinction coefficient of 26 000 $\text{M}^{-1} \text{cm}^{-1}$ was used to calculate product formation. For the reactions that tested the potency of the hydrazino-Lys-4 H3-21 and H3(1–21)K4azaK peptide inhibitors, reactions contained 50 mM HEPES buffer (pH 7.5), 0.76 μM horseradish peroxidase, 600 μM substrate (H3(1-21)K4Kme2), 320 nM GST-LSD1, and 0.1 mM Amplex Red (used to achieve improved sensitivity due to high potency). Absorbance changes were monitored at 571 nm, and an extinction coefficient of 52 000 $\text{M}^{-1} \text{cm}^{-1}$ was used to calculate product formation. The progress curves obtained in the presence of the peptide inhibitors were fit to the following single

exponential for slow-binding inhibitors which assumes a steady-state velocity of zero:⁷⁶

$$\text{Product} = v_0(1 - e^{-kt})/k + \text{offset} \quad (1)$$

The k_{obs} values were then analyzed by the method of Kitz and Wilson analysis⁷⁷ to yield k_{inact} and $K_{\text{i(inact)}}$ using the following equations:

$$k_{\text{obs}} = (k_{\text{inact}}*[I])/(K_{\text{i(inact)}} + [I]) \quad (2)$$

$K_{\text{i(inact)}}$ was extrapolated to zero substrate by:

$$K_{\text{i(inact)}}^{\text{app}} = K_{\text{i(inact)}}(1 + [S]/K_{\text{m}}) \quad (3)$$

■ ASSOCIATED CONTENT

📄 Supporting Information

Supplemental mass spectrometric analyses, structural diagrams, inhibition data, HPLC chromatograms, NMR spectra and complete ref 29. This material is available free of charge via the Internet at <http://pubs.acs.org>.

■ AUTHOR INFORMATION

✉ Corresponding Author

pcole@jhmi.edu

Notes

The authors declare no competing financial interest.

■ ACKNOWLEDGMENTS

We thank William Hawse and Cynthia Wolberger for providing the Sir2Tm expression plasmid, Robert Cole and the Mass Spectrometry and Proteomics Facility at the Johns Hopkins School of Medicine for the use of the MALDI-TOF instrument, the Johns Hopkins Biomolecular NMR Center for providing NMR resources and facilities, David Meyers, Marc Holbert, Kannan Karukurichi, Yousang Hwang, Youg-Hoon Ahn, and Weiping Zheng for helpful discussion. We are grateful for support from the NIH.

■ REFERENCES

- (1) Walsh, C. *Posttranslational Modification of Proteins: Expanding Nature's Inventory*; Roberts and Co. Publishers: Englewood, CO., 2006.
- (2) Cole, P. A. *Nat. Chem. Biol.* **2008**, *4*, 590.
- (3) Bannister, A. J.; Kouzarides, T. *Cell Res.* **2011**, *21*, 381.
- (4) Thompson, P. R.; Fast, W. *ACS Chem. Biol.* **2006**, *1*, 433.
- (5) Kouzarides, T. *Cell* **2007**, *128*, 693.
- (6) Li, M.; Luo, J.; Brooks, C. L.; Gu, W. *J. Biol. Chem.* **2002**, *277*, 50607.
- (7) Rodriguez, M. S.; Desterro, J. M.; Lain, S.; Lane, D. P.; Hay, R. T. *Mol. Cell Biol.* **2000**, *20*, 8458.
- (8) Shi, X.; Kachirskaja, I.; Yamaguchi, H.; West, L. E.; Wen, H.; Wang, E. W.; Dutta, S.; Appella, E.; Gozani, O. *Mol. Cell* **2007**, *27*, 636.
- (9) Kruse, J. P.; Gu, W. *Cell* **2008**, *133*, 930.
- (10) Rust, H. L.; Thompson, P. R. *ACS Chem. Biol.* **2011**, *6*, 881.
- (11) Vidal, C. J. *Post-Translational Modifications in Health and Disease*; Springer: New York, 2011.
- (12) Alcain, F. J.; Villalba, J. M. *Expert Opin. Ther. Pat.* **2009**, *19*, 283.
- (13) Bolden, J. E.; Peart, M. J.; Johnstone, R. W. *Nat. Rev. Drug Discovery* **2006**, *5*, 769.
- (14) Dekker, F. J.; Haisma, H. J. *Drug Discovery Today* **2009**, *14*, 942.
- (15) Haberland, M.; Montgomery, R. L.; Olson, E. N. *Nat. Rev. Genet.* **2009**, *10*, 32.
- (16) Kim, H. J.; Bae, S. C. *Am. J. Transl. Res.* **2011**, *3*, 166.
- (17) Mahajan, S. S.; Leko, V.; Simon, J. A.; Bedalov, A. *Handb. Exp. Pharmacol.* **2011**, *206*, 241.
- (18) Sauve, A. A. *Biochim. Biophys. Acta* **2010**, *1804*, 1591.

- (19) de Ruijter, A. J.; van Gennip, A. H.; Caron, H. N.; Kemp, S.; van Kuilenburg, A. B. *Biochem. J.* **2003**, *370*, 737.
- (20) Glozak, M. A.; Sengupta, N.; Zhang, X.; Seto, E. *Gene* **2005**, *363*, 15.
- (21) Smith, B. C.; Hallows, W. C.; Denu, J. M. *Chem. Biol.* **2008**, *15*, 1002.
- (22) Sauve, A. A.; Wolberger, C.; Schramm, V. L.; Boeke, J. D. *Annu. Rev. Biochem.* **2006**, *75*, 435.
- (23) Choudhary, C.; Kumar, C.; Gnad, F.; Nielsen, M. L.; Rehman, M.; Walther, T. C.; Olsen, J. V.; Mann, M. *Science* **2009**, *325*, 834.
- (24) Haigis, M. C.; Guarente, L. P. *Genes Dev.* **2006**, *20*, 2913.
- (25) Kruszewski, M.; Szumiel, I. *DNA Repair* **2005**, *4*, 1306.
- (26) Li, X.; Kazgan, N. *Int. J. Biol. Sci.* **2011**, *7*, 575.
- (27) Dokmanovic, M.; Clarke, C.; Marks, P. A. *Mol. Cancer Res.* **2007**, *5*, 981.
- (28) Emanuele, S.; Lauricella, M.; Tesoriere, G. *Int. J. Oncol.* **2008**, *33*, 637.
- (29) Lara, E.; et al. *Oncogene* **2009**, *28*, 781.
- (30) Wagner, J. M.; Hackanson, B.; Lubbert, M.; Jung, M. *Clin. Epigenetics* **2010**, *1*, 117.
- (31) Cen, Y.; Sauve, A. A. *J. Am. Chem. Soc.* **2010**, *132*, 12286.
- (32) French, J. B.; Cen, Y.; Sauve, A. A. *Biochemistry* **2008**, *47*, 10227.
- (33) Sauve, A. A.; Schramm, V. L. *Curr. Med. Chem.* **2004**, *11*, 807.
- (34) Sauve, A. A.; Schramm, V. L. *Biochemistry* **2003**, *42*, 9249.
- (35) Hu, P.; Wang, S.; Zhang, Y. *J. Am. Chem. Soc.* **2008**, *130*, 16721.
- (36) Smith, B. C.; Denu, J. M. *J. Am. Chem. Soc.* **2007**, *129*, 5802.
- (37) Hirsch, B. M.; Zheng, W. *Mol. Biosyst.* **2011**, *7*, 16.
- (38) Huang, R.; Holbert, M. A.; Tarrant, M. K.; Curtet, S.; Colquhoun, D. R.; Dancy, B. M.; Dancy, B. C.; Hwang, Y. S.; Tang, Y.; Meeth, K.; Marmorstein, R.; Cole, R. N.; Khochbin, S.; Cole, P. A. *J. Am. Chem. Soc.* **2010**, *132*, 9986.
- (39) Huhtiniemi, T.; Suuronen, T.; Lahtela-Kakkonen, M.; Bruijn, T.; Jaaskelainen, S.; Poso, A.; Salminen, A.; Leppanen, J.; Jarho, E. *Bioorg. Med. Chem.* **2010**, *18*, 5616.
- (40) Jamonnak, N.; Fatkins, D. G.; Wei, L.; Zheng, W. *Org. Biomol. Chem.* **2007**, *5*, 892.
- (41) Jamonnak, N.; Hirsch, B. M.; Pang, Y.; Zheng, W. *Bioorg. Chem.* **2010**, *38*, 17.
- (42) Li, F.; Allahverdi, A.; Yang, R.; Lua, G. B.; Zhang, X.; Cao, Y.; Korolev, N.; Nordenskiold, L.; Liu, C. F. *Angew. Chem., Int. Ed.* **2011**, *50*, 9611.
- (43) Fatkins, D. G.; Monnot, A. D.; Zheng, W. *Bioorg. Med. Chem. Lett.* **2006**, *16*, 3651.
- (44) Hawse, W. F.; Hoff, K. G.; Fatkins, D. G.; Daines, A.; Zubkova, O. V.; Schramm, V. L.; Zheng, W.; Wolberger, C. *Structure* **2008**, *16*, 1368.
- (45) Smith, B. C.; Denu, J. M. *Biochemistry* **2007**, *46*, 14478.
- (46) Huang, J.; Berger, S. L. *Curr. Opin. Genet. Dev.* **2008**, *18*, 152.
- (47) Huang, J.; Sengupta, R.; Espejo, A. B.; Lee, M. G.; Dorsey, J. A.; Richter, M.; Opravil, S.; Shiekhatar, R.; Bedford, M. T.; Jenuwein, T.; Berger, S. L. *Nature* **2007**, *449*, 105.
- (48) Forneris, F.; Battaglioli, E.; Mattevi, A.; Binda, C. *FEBS J.* **2009**, *276*, 4304.
- (49) Forneris, F.; Binda, C.; Battaglioli, E.; Mattevi, A. *Trends Biochem. Sci.* **2008**, *33*, 181.
- (50) Culhane, J. C.; Wang, D.; Yen, P. M.; Cole, P. A. *J. Am. Chem. Soc.* **2010**, *132*, 3164.
- (51) Szewczuk, L. M.; Culhane, J. C.; Yang, M.; Majumdar, A.; Yu, H.; Cole, P. A. *Biochemistry* **2007**, *46*, 6892.
- (52) Rodriguez, M.; Taddei, M. *Synthesis* **2005**, 493.
- (53) Fina, N. J.; Edwards, J. O. *Int. J. Chem. Kinet.* **1973**, *5*, 1.
- (54) Calabretta, R.; Gallina, C.; Giordano, C. *Synthesis* **1991**, 536.
- (55) Kison, C.; Meyer, N.; Opatz, T. *Angew. Chem., Int. Ed.* **2005**, *44*, 5662.
- (56) Elamin, B.; Anantharamaiah, G. M.; Royer, G. P.; Means, G. E. *J. Org. Chem.* **1979**, *44*, 3442.
- (57) Fahie, K.; Hu, P.; Swatkoski, S.; Cotter, R. J.; Zhang, Y.; Wolberger, C. *FEBS J.* **2009**, *276*, 7159.
- (58) Hawse, W. F.; Wolberger, C. *J. Biol. Chem.* **2009**, *284*, 33654.
- (59) Kowieski, T. M.; Lee, S.; Denu, J. M. *J. Biol. Chem.* **2008**, *283*, 5317.
- (60) Lee, S. E.; Elphick, L. M.; Anderson, A. A.; Bonnac, L.; Child, E. S.; Mann, D. J.; Gouverneur, V. *Bioorg. Med. Chem. Lett.* **2009**, *19*, 3804.
- (61) Reddy, D. N.; Thirupathi, R.; Prabhakaran, E. N. *Chem. Commun. (Cambridge, U.K.)* **2011**, *47*, 9417.
- (62) Culhane, J. C.; Cole, P. A. *Curr. Opin. Chem. Biol.* **2007**, *11*, 561.
- (63) Erikson, J. M.; Prough, R. A. *J. Biochem. Toxicol.* **1986**, *1*, 41.
- (64) Baker, G. B.; Sowa, B.; Todd, K. G. *J. Psychiatry Neurosci.* **2007**, *32*, 313.
- (65) Gillman, P. K. *J. Clin. Psychopharmacol.* **2011**, *31*, 66.
- (66) Binda, C.; Valente, S.; Romanenghi, M.; Pilotto, S.; Cirilli, R.; Karytinis, A.; Ciossani, G.; Botrugno, O. A.; Forneris, F.; Tardugno, M.; Edmondson, D. E.; Minucci, S.; Mattevi, A.; Mai, A. *J. Am. Chem. Soc.* **2010**, *132*, 6827.
- (67) Culhane, J. C.; Szewczuk, L. M.; Liu, X.; Da, G.; Marmorstein, R.; Cole, P. A. *J. Am. Chem. Soc.* **2006**, *128*, 4536.
- (68) Huang, Y.; Stewart, T. M.; Wu, Y.; Baylin, S. B.; Marton, L. J.; Perkins, B.; Jones, R. J.; Woster, P. M.; Casero, R. A. *Jr. Clin. Cancer Res.* **2009**, *15*, 7217.
- (69) Lee, M. G.; Wynder, C.; Schmidt, D. M.; McCafferty, D. G.; Shiekhatar, R. *Chem. Biol.* **2006**, *13*, 563.
- (70) Mimasu, S.; Umezawa, N.; Sato, S.; Higuchi, T.; Umehara, T.; Yokoyama, S. *Biochemistry* **2010**, *49*, 6494.
- (71) Schmidt, D. M.; McCafferty, D. G. *Biochemistry* **2007**, *46*, 4408.
- (72) Yang, M.; Culhane, J. C.; Szewczuk, L. M.; Jalili, P.; Ball, H. L.; Machius, M.; Cole, P. A.; Yu, H. *Biochemistry* **2007**, *46*, 8058.
- (73) Smith, J. S.; Avalos, J.; Celic, I.; Muhammad, S.; Wolberger, C.; Boeke, J. D. *Methods Enzymol.* **2002**, *353*, 282.
- (74) Laemmli, U. K. *Nature* **1970**, *227*, 680.
- (75) Taverna, S. D.; Ueberheide, B. M.; Liu, Y.; Tackett, A. J.; Diaz, R. L.; Shabanowitz, J.; Chait, B. T.; Hunt, D. F.; Allis, C. D. *Proc. Natl. Acad. Sci. U.S.A.* **2007**, *104*, 2086.
- (76) Copeland, R. A. *Enzymes: A Practical Introduction to Structure, Mechanism, and Data Analysis*; 2nd ed.; Wiley: New York, 2000.
- (77) Kitz, R.; Wilson, I. B. *J. Biol. Chem.* **1962**, *237*, 3245.